Conclusions of a Cryogenic Motor Configuration Study for Aircraft Propulsion

Justin J. Scheidler
Rotating and Drive Systems Branch
NASA Glenn Research Center
Cleveland, USA
justin.j.scheidler@nasa.gov

Aaron D. Anderson
Diagnostics and Electromagnetics Branch
NASA Glenn Research Center
Cleveland, USA
aaron.d.anderson-1@nasa.gov

Thomas F. Tallerico
Rotating & Drive Systems Branch
NASA Glenn Research Center
Cleveland, USA

***Abstract*— Cryogenic electric machines are a promising technology for multi megawatt electrified aircraft propulsion systems. This paper shares the lessons learned from a design study that evaluated several configurations of a 5 MW cryogenic motor for this application. The lessons are drawn from a qualitative study of 17 configurations and a quantitative study of 8 down selected configurations. The quantitative study involved using analytical calculations (electromagnetic, thermofluid, mechanical, and motor sizing) to determine each configuration's Pareto front of total efficiency and total specific power. The two highest performing configurations – one with a permanent magnet rotor and one with a superconducting rotor – are compared in terms of performance and several practical criteria. One motor configuration is down selected for future detailed design and demonstration at the multi megawatt level. An assessment of different stator coolants is also presented.**

Keywords—electrified aircraft propulsion, electric machines, cryogenics, superconductivity

I. Introduction

Research and development in aviation propulsion is striving to achieve economic benefits (reduced fuel consumption, decreased energy costs and increased cost stability, maintaining the United States' competitiveness, and reinvigorating existing aircraft markets), societal benefits (growth in the global access to air travel), and environmental benefits (reduced impact on climate and improved air quality). Electrified propulsion systems are an attractive approach to enable more fuel-efficient aircraft, in part by leveraging advanced engine cycles. Electrified propulsion relies on electric machines to generate electricity and drive fans that produce thrust. Multi megawatt machines are required for transport-class aircraft, which carry about 150 or more passengers and dominate the market. At this power level, electric machines with cryogenic stators are a promising technology to achieve the very high efficiency and specific power demanded by this application. Electric machines with superconducting stators have been under development for decades [1] and have received significant attention in recent years for electrified aircraft applications [2][8]. However, cryogenic stators with non-superconducting metallic conductors have received limited attention for these applications as they are frequently dismissed in favor of superconductors (SC). A number of conductor comparison papers have been completed that motivate the use of superconductors for cryogenic stators [9][12]. These studies, however, often compare normal and superconducting stators excited by the same magnetic field and do not complete comparisons at the full machine design level. Also, an extensive assessment of motor configurations is unavailable. This paper summarizes a thorough design study of 5 MW motors with cryogenic stators. Both superconductors and non-superconductors are considered as the stator conductor. The motor's efficiency and total specific power are optimized for several combinations of motor configuration, stator coolant, and stator conductor. This paper is a significant update and extension of the previously published preliminary assessment [13],[14]. This paper provides a final quantitative assessment of the motor configurations along with a complete discussion of the results and down select of one configuration.

II. Motor Specifications

NASA's superconducting 'vision' motor is constrained to be a 5 MW motor that spins at 1,500 to 3,000 rpm (to directly drive a propeller) and has a cryogenic stator that is excited by an inverter driven by a $\leq \pm 1{,}000$ V DC bus. Modest goals for specific power were defined (20 kW/kg goal, 30 kW/kg stretch goal), because TRL advancement of cryogenic machine technology is emphasized over performance optimization. The efficiency goals are explained in the subsection below. The remaining specifications are as defined in [14].

A. Motor Efficiency Specification

The majority of a motor's power loss is generated in its stator. Thus, a motor with a cryogenic stator must have high efficiency to ensure that the cryogenic cooling system can have a manageable size and mass and that it is feasible to achieve a small temperature gradient within the stator winding. There is also a desire to ensure the developed motor is compatible with potential future aircraft with hydrogen-burning engines (i.e., that the motor's cryogenic heat load can be dissipated into the fuel without requiring more liquid hydrogen than the engine needs). Accordingly, an estimate of the required motor efficiency was

This work was supported by the NASA Subsonic Vehicle Technologies and Tools Project within NASA's Aeronautics Research Mission Directorate.

derived using the estimated performance and specifications of a future engine developed to burn hydrogen along with the assumption of a turboelectric powertrain with DC power distribution where the generator, power electronics, and motor have equal efficiency. The result is depicted in Fig. 1. In this case, the maximum take off condition is found to be more demanding than cruise. Increased electrification of the propulsion system is often predicted by aircraft analyses to provide reduced fuel consumption. Thus, a motor efficiency goal of 99.5% and a stretch goal of 99.8% were chosen.

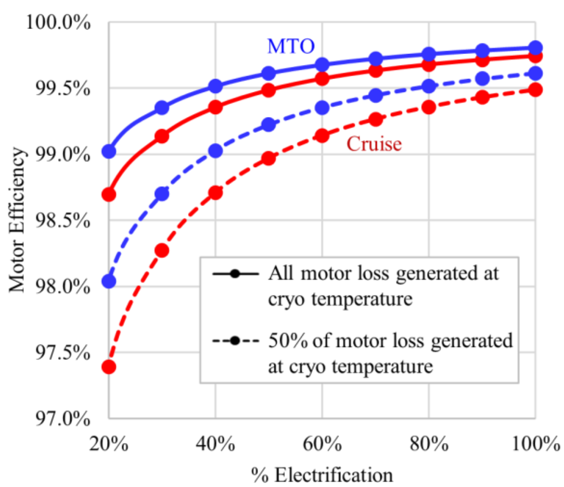

Fig. 1. Estimate of the required motor efficiency to avoid extra cryocooling in a notional ~150 passenger liquid hydrogen fueled aircraft with an advanced hydrogen burning engine as a function of how much the propulsion system is electrified; Results shown for maximum take off (MTO) and cruise conditions and for half or all of the motor's loss being generated at cryogenic temperature.

III. Motor Configurations and Methodology

A motor's configuration defines how it functions and what the motor looks like, including the operating mechanism, stator type, rotor type, magnetic flux direction, and the basic construction. This study considered a wide range of synchronous motors with a cryogenic stator (either metallic or superconducting). Of the 17 configurations evaluated, 9 have a permanent magnet (PM) rotor and 8 have a high temperature superconducting (HTS) rotor. Radial, axial, and combined radial and axial flux directions were included. Multiple motor constructions were examined, including variations in stator winding type (distributed, concentrated, or 'zig-zag' [15]), number of stators and rotors and their location, and locations of vacuum vessel and rotor. As described in [14], a down select to 8 configurations was made based on a qualitative assessment of each motor in terms of 9 criteria covering electromagnetic, thermal, structural, and rotordynamics attributes. Five motors with a PM rotor were chosen for further study: a radial flux outer rotor with the stator or rotor containing the vacuum, a radial flux 'Helmholtz' motor (see appendix for a description), an axial flux motor in a rotor-stator-rotor (R-S-R) construction with the stator containing the vacuum, and a 3-rotor radial+axial flux motor with no iron. Three motors with a HTS rotor were chosen for further study: a radial flux inner rotor and an axial flux motor with 'zig-zag' winding in a R-S-R or stator-rotor-stator (S-R-S) construction.

Further study of the 8 selected configurations used a genetic algorithm to find Pareto optimal fronts of each of the configurations. The two fitness parameters were overall efficiency and total specific power (i.e., relative to total mass, not electromagnetic mass). Fitness was calculated using analytical sizing and modeling equations, see Fig. 2 for the flow of calculation steps. The analysis and models are similar to [13],[14] with some refinement and errors corrected. The key changes include:

- DC bus voltage changed from ±270 V to ±1,000 V
- Equivalent tip speeds changed from 79 to 94 m/s to 100 m/s
- Coolant changed from liquid neon to gaseous helium, as described in Section IV.

Details specific to the Helmholtz configuration will be presented in future work.

The electromagnetic analysis included calculation of steady-state fields for a range of rotor positions. The fields produced by permanent magnets were calculated using analytical equations for Halbach arrays [16],[17] whereas those produced by each conductor in the rotor and stator coils were calculated using the analytical equation for field produced by a thin, infinitely long wire. Stator sizing via Essen's rule was conducted assuming a 10% margin on torque. For superconducting coils, a safety factor of at least 1.5 is maintained above the critical current, which takes into account temperature-, magnetic field strength-, and magnetic field direction-dependence. The stator coil design includes defining the number of turns so that the peak-to-peak back emf is at most 80% to 90% of the bus voltage span (i.e., 2,000 V) and geometric constraints to ensure an integer number of turns and the HTS is commercially available. The Litz wire bundle was designed as in [13].

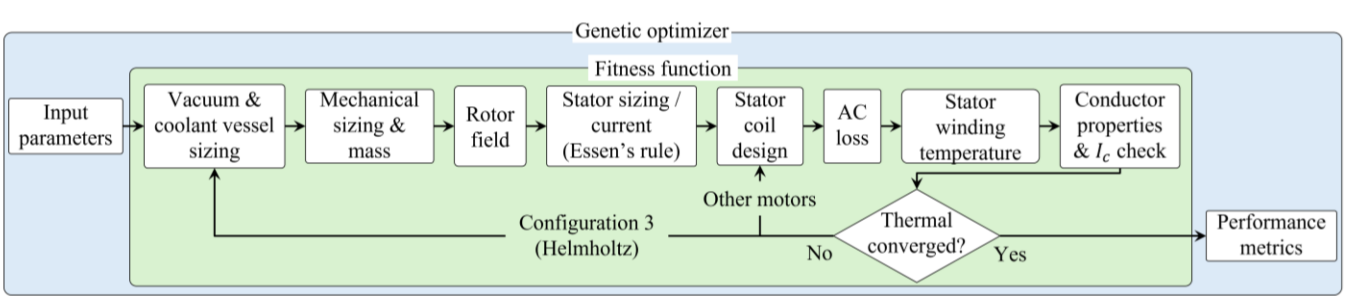

Fig. 2. Flow chart of the motor design code that depicts the key calculations; I_c is the superconductor's critical current.

Losses considered in the code include the following (note that some are not applicable to every configuration):

- In metallic Litz wire: DC conduction, AC skin effect, and proximity losses – each time dependent
- In superconductors: hysteresis, eddy current, coupling, and transport (in HTS) losses – each time dependent
- Bearing loss
- Windage loss (only in Helmholtz)
- Power to pump coolant through the motor
- Cryocooler power (using trends from existing cryocoolers)
- Iron loss (Steinmetz equations using calculated fields)
- Rotary vacuum seal drag (fixed at 1.5 kW)

Mechanical sizing considers static strength of mechanical components assuming simplified geometry consisting of discs, cylinders, etc. Sizing considers pressure loads on vacuum and fluid containment vessels, torque loads, centrifugal loading, and gyroscopic loading from a propellor. The wall thicknesses of each pressure vessel are sized for hoop stress or buckling as appropriate for each configuration. Bearings are selected from a catalog of existing bearings and sized for 90% reliability at 5,000 hours life.

Mechanical components located within magnetic fields are made of G-10 fiberglass composite to avoid eddy current losses. The shaft is sized using 17-4 stainless steel. Other structures are made of Ti-6Al-4V. For Litz wires, strand insulation is polyimide with meta-aramid (Nomex) insulation around bundles of strands. Litz wires are potted with a filled epoxy having a thermal conductivity of 1.45 W/m-K.

The motor's total mass is calculated, including active electromagnetic components, shafts, bearings, vacuum vessels, cooling fluid containment vessels, rotor structures, stator structures, cryocooler and the thermal connections to it (for designs with HTS rotors), and a 10 kg allowance for fasteners and other miscellaneous components not explicitly modeled.

Thermal modeling is based on time-averaged losses. Stator windings are assumed to be directly cooled with coolant channels in-slot on one or two faces of the winding (e.g., at the inside and/or outside diameter in radial flux motors), based on feasibility for each configuration. Thermal analysis differs slightly between the Helmholtz configuration and all others. For most configurations, thermal analysis is based on a 1D model using a homogenized thermal resistance for the winding area and the coolant temperature at the motor's outlet. For the Helmholtz configuration, the losses in each HTS tape (circumferential direction) are calculated and temperatures are modeled along the width (aligned radially) of each HTS tape resulting in a semi-2D thermal model; in this configuration, the coolant temperature at the motor's inlet is used. As shown in Fig. 2, the loss calculations and thermal analysis is iterated until (a) the temperatures and the superconducting coil's critical current converge (i.e., a valid design) or (b) the temperature is too high or critical current is zero (i.e., an invalid design).

IV. Results and Lessons Learned

The results in this paper were obtained for a ±1,000 V DC bus and a 100 m/s equivalent tip speed [14]. Each result in this section assumed a speed of 3,000 rpm.

Each configuration could be evaluated for a range of stator conductors, stator coolants, and coolant temperatures. A preliminary assessment of stator conductors in multiple motor configurations indicated that copper Litz wire with 50 AWG strands outperforms two superconductors (MgB2 and Bi-2212) and high purity aluminum when the stator is cooled using liquid neon at 25 K. This finding will be further investigated and then published in future work. In this paper, only results for copper Litz with 50 AWG strands are shown, except for the Helmholtz configuration, which performs best with a high temperature superconducting (REBCO) stator. Results for 45 AWG were also obtained but are not shown because they are very similar in nearly every case (i.e., the negative impact of larger strand diameters on AC loss and motor performance was often minimal until the strand gauge was reduced below 45 AWG).

To select a stator coolant, the radial flux inner HTS rotor configuration was separately optimized for different subcooled cryogenic liquids and gaseous helium. Although liquid hydrogen is not considered a viable candidate for in-motor cooling on an aircraft, it was included for comparison purposes. The Pareto front for each coolant is shown in Fig. 3. Unsurprisingly, liquid cryogens enable higher performance at a given temperature, particularly near the upper limit of specific power, which is strongly influenced by thermal management. However, gaseous helium provides similar performance at locations on the Pareto front away from the specific power limit. Consequently, helium was selected due to its interest from industry, its much lower density, and practical benefits (no phase change [and accompanying large volume change] due to over temperature events, no potential for cavitation damage or cavitation instability [18]). The results below assume gaseous helium coolant with a temperature of 35 K at the motor inlet,

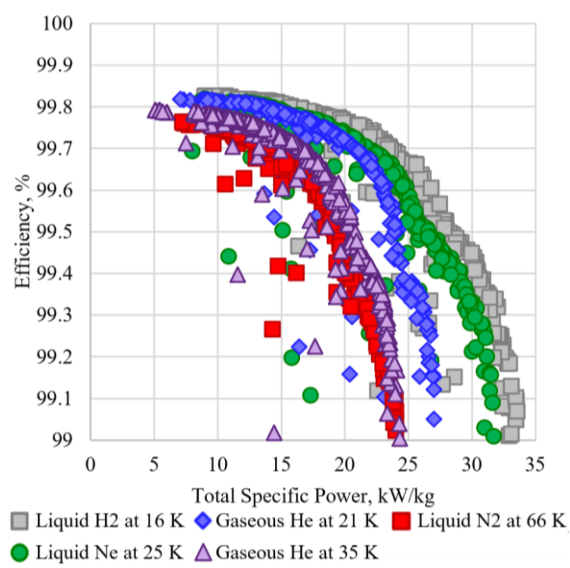

Fig. 3. Optimization results for the radial flux motor with inner HTS rotor and copper Litz wire (Cu) stator for different stator coolants.

which was chosen to be conservative in the case where liquid hydrogen is available as the ultimate heat sink.

A. Configurations with Permanent Magnet Rotors

The optimization result for each motor configuration with a PM rotor is given in Fig. 4. Note that the efficiency of the outer rotor and 3-rotor configurations is artificially high by about 0.01% to 0.03% because windage loss was neglected in those cases. The axial flux configuration did not close due to the large air gaps caused by the thickness of the G-10 vacuum and fluid containment vessels needed to avoid buckling. To facilitate analytical calculation, these vessels were assumed to be composed of simple discs. Vessels with a stiffer geometry would lessen the problem and are worth investigation, although they aren't expected to enable that configuration to approach the goal efficiency and specific power. Motors with permanent magnet rotors and cryogenic Litz wire stators can achieve very high efficiency (> 99.8%) but only modest specific power (< 15 kW/kg). The outer rotor and 3-rotor configurations don't meet the goal largely because the rotor-produced field in the stator is relatively low, which necessitates a relatively high phase current that causes higher loss and degrades thermal management. The Helmholtz motor clearly outperforms the other configurations with a PM rotor and approximately matches the goal. The Helmholtz Pareto front is less populated for the defined specifications and performance regime of interest. This may suggest that it has a smaller design space and greater sensitivity to changes in constraints or material properties, although the allowed geometry of the Helmholtz stator is more discrete than the other configurations due to the width of commercially available HTS. None of the motors are predicted to approach the stretch goal.

For each of these configurations, the permanent magnets constitute a significant fraction of the motor's total mass. On the Pareto fronts at an efficiency of 99.4% or higher, the mass of magnets in the Helmholtz motor (about 100 to 150 kg) and outer rotor motors (about 250 to 375 kg) is about 45% to 55% of the total mass; that fraction increases to about 60% to 70% of the total mass in the 3-rotor motor (about 200 to 475 kg). Although the motor design codes include an upper limit on the thickness of the magnets in the motor's flux direction, the fidelity of the constraint should be improved in future work to verify that impractical designs are eliminated.

The Helmholtz configuration was carried forward as a configuration finalist based on its performance.

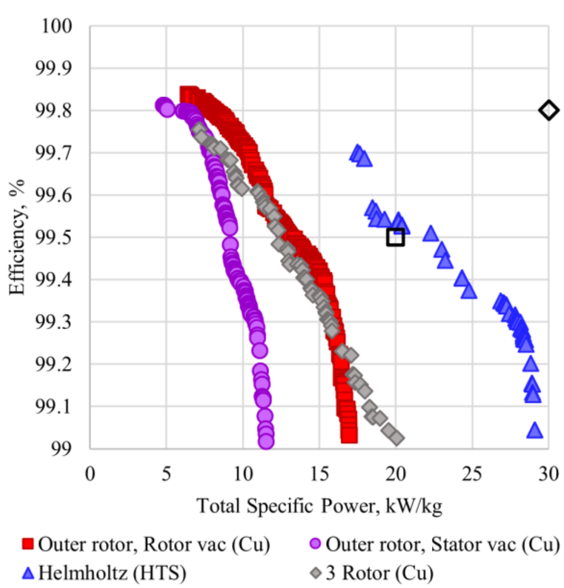

Fig. 4. Optimization results for the configurations with permanent magnet rotors; results shown for GHe coolant at ≥35 K and copper Litz wire (Cu) stators except for the Helmholtz, which uses high temperature superconductor (HTS). The goal and stretch goal are shown by the black square and black diamond, respectively.

B. Configurations with Superconducting Rotors

The optimization result for each motor configuration with a HTS rotor is given in Fig. 5. The performance of the axial flux motors with a HTS rotor is limited by the assumed geometry and stiffness of the fluid containment vessel, as explained above. The R-S-R axial configuration did not close as a result. The S-R-S axial configuration outperforms the R-S-R one because (a) the heat load on the single rotor is smaller and the rotor field on each side of the rotor produces torque and (b) each of its two stators can be somewhat thinner and easier to cool. The radial flux inner rotor configuration has a somewhat smaller upper limit on efficiency but can achieve much higher specific power.

The radial flux inner rotor configuration was carried forward as a configuration finalist based on its performance.

V. Motor Configuration Selection

To down select between the two configuration finalists, each was optimized for a speed of 1,500 rpm. The Pareto front of each motor at both 1,500 rpm and 3,000 rpm is shown in Fig. 6. At 3,000 rpm, the two motors have equivalent performance (considering the low to moderate fidelity of the design code) in the vicinity of the efficiency and specific power goal. The radial

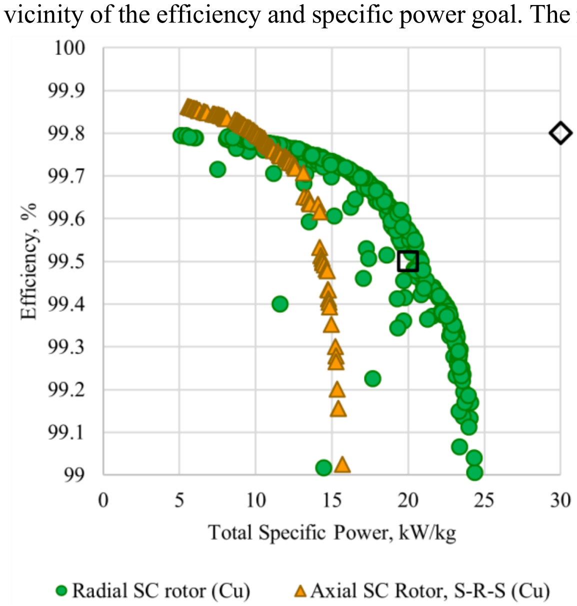

Fig. 5. Optimization results for the configurations with superconducting rotors; results shown for GHe coolant at ≥35 K and copper Litz wire (Cu) stators. The goal and stretch goal are shown by the black square and black diamond, respectively.

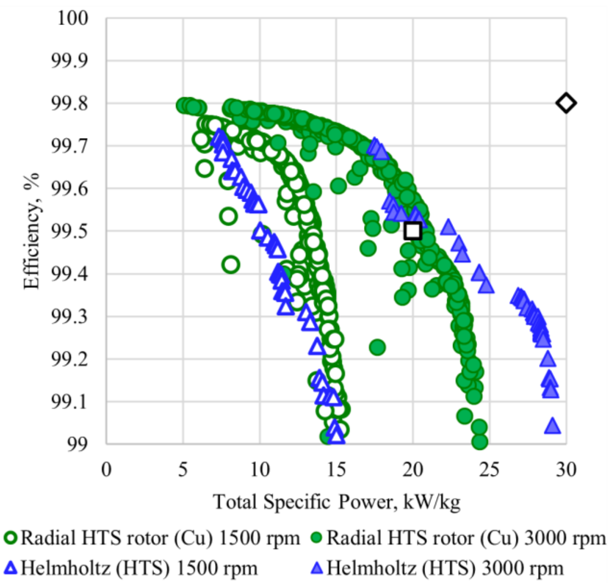

Fig. 6. Optimization results for the configuration finalists at the specified operating speed bounds; results shown for GHe coolant at ≥35 K and copper Litz wire (Cu) or high temperature superconducting (HTS) stators. The goal and stretch goal are shown by the black square and black diamond, respectively.

flux inner HTS rotor configuration is found to scale to lower speed better than the Helmholtz PM motor. However, the performance difference is small enough that additional factors needed to be weighed before selecting the configuration to develop and demonstrate.

Table 1 presents a qualitative comparison of the motor configuration finalists across a range of criteria. The radial flux Helmholtz motor is novel, offers benefits to the motor and inverter based on its lack of cryogenic rotor cooling, and enables use of the highest performance conductor in the stator. However, it introduces mechanical challenges due to its sandwiched stator and is less mature, which causes higher uncertainty (particularly in AC loss predictions). The radial flux motor with an inner HTS rotor is more mature and leverages prior work and has fewer thermal management and mechanical challenges in the stator due to its geometry and lower cryogenic heat load. However, it introduces thermal and mechanical challenges on the rotor due to its cryogenic temperature.

Collectively, both configurations are competitive and worthy of selection but for different reasons. After considering the information presented herein, the project's risk tolerance, and additional internal factors, the NASA team chose to select the radial flux inner HTS rotor configuration for detailed design. One deciding factor was the relatively high uncertainty in AC loss predictions for the Helmholtz configuration. This quantitative and qualitative comparison will be revisited and expanded upon at the conclusion of the project, taking into account lessons learned and forthcoming AC loss data.

VI. Conclusions

This paper summarized the results and conclusions of an investigation into the preferred configuration of a 5 MW 'vision' motor with cryogenic stator for directly driving the propellers of an electrified aircraft. Eight configurations were down selected

TABLE I. Comparison of the Motor Configuration Finalists.

Criteria	Radial Helmholtz motor with PM rotor	Radial inner HTS rotor
Can meet technical objectives	Yes	Yes
Stator conductor	Better performance with HTS	Better performance with Cu Litz
Input to community	Novel architecture development REBCO AC loss performance	Cryogenic Cu Litz performance Cryocooler development Rotary power transfer development
Key challenges	Assembly of large PMs Vacuum vessel in air gap Cantilevered rotor & stator Packaging of stator feedthroughs	Needs rotor cryocooling Needs power transfer onto rotor May need rotary vacuum seal(s) May need vacuum vessel / magnetic shield in air gap
Key benefits	Simpler rotor cooling Relaxed inverter output distortion limit	Lower cryogenic heat load Reduced structural complexity & better rotordynamics
Bottom line	Novel architecture that enables ideal SC in stator Less mature, higher uncertainty	Established architecture Leverages prior work

from a wide range of synchronous options based on a qualitative assessment. The performance limit of those eight was obtained using an analytical motor design code that optimizes for efficiency and total specific power. A speed of 3,000 rpm and gaseous helium coolant at ≥ 35 K were assumed. One motor with a PM rotor and one with a HTS rotor were chosen as finalists. The finalists were compared in terms of their performance at two speeds and characteristics. A radial flux motor with inner HTS rotor was selected.

This project will continue by conducting the detailed design of a ~2 MW radial flux motor with HTS rotor – termed the Cryogenic High-power Integrated Low Loss (CHILL) motor. The CHILL motor will be built, paired with a CHILL drive also in development at NASA Glenn Research Center, and then tested at full power.

References

[1] K. S. Haran et al., "High power density superconducting rotating machines—development status and technology roadmap," Supercond. Sci. Technol., vol. 30, no. 12, 2017.

[2] Y. Terao, A. Seta, H. Ohsaki, H. Oyuri and N. Morioka, "Lightweight design of fully superconducting motors for electrical aircraft propulsion systems," IEEE Trans. Appl. Supercond., vol. 29, no. 5, 2019.

[3] Y. Terao, Y. Ishiba, H. Ohsaki, K. Okai and H. Taguchi, "Partial load analysis of turbo electric propelling fans using superconducting motors," in AIAA Propulsion and Energy Forum, Virtual, 2021.

[4] J. Voccio and J. Tangudu, "Design and evaluation of a high power density 5 MW, 6000 RPM fully-superconducting generator," in Elec. Aircraft Tech. Symp., Virtual, 2020.

[5] H. Sasa et al., "Experimental evaluation of 1 kW-class prototype REBCO fully superconducting synchronous motor cooled by subcooled liquid nitrogen for E-aircraft," IEEE Trans. Appl. Supercond., vol. 31, no. 5, 2021.

[6] J. K. Noland, R. Mellerud and C. Hartmann, "Next-generation cryo-electric hydrogen-powered aviation: a disruptive superconducting

propulsion system cooled by onboard cryogenic fuels," IEEE Indus. Electron. Magazine, vol. 16, no. 4, pp. 6-15, 2022.

[7] M. Corduan, M. Boll, R. Bause, M. P. Oomen, M. Filipenko and M. Noe, "Topology comparison of superconducting AC machines for hybrid electric aircraft," IEEE Trans. Appl. Supercond., vol. 30, no. 2, 2020.

[8] G. V. Brown, "Weights and efficiencies of electric components of a turboelectric aircraft propulsion system," in 49th AIAA Aerospace Sci. Meeting, Orlando, FL, 2011.

[9] M. D. Sumption, J. Murphy, M. Susner and T. Haugan, "Performance metrics of electrical conductors for aerospace cryogenic motors, generators, and transmission cables," Cryogenics, vol. 111, 2020.

[10] J. Kwon et al., "AC loss of various conductors for power cables, busbars, motor windings in cryogenic electric aircraft," in AIAA AVIATION Forum & ASCEND, Las Vegas, NV, 2024.

[11] G. V. Brown, J. J. Trudell, L. W. Kohlman, K. P. Duffy and F. D. Koci, "Status of analysis and manufacturability of superconducting wires with low AC losses," NASA/TM-20205005815, 2020.

[12] H. J. Kwon, M. D. Sumption, J. Hauhan and E. Collings, "High purity aluminum in cryogenic motors for electric aircraft," in AIAA AVIATION Forum, San Diego, CA, 2023.

[13] T. F. Tallerico, J. J. Scheidler, and A. D. Anderson, "Cryogenic copper and aluminum Litz wire motors for electric aircraft," in 2025 IEEE/AIAA Transport. Electrification Conf. and Elec. Aircraft Tech. Symp. (ITEC+EATS), Anaheim, CA, 2025.

[14] J. J. Scheidler, T. F. Tallerico, A. D. Anderson, and P. E. Kascak, " Motor configuration trade study for a new technical challenge to develop a 5 MW cryogenic motor and drive," [available online https://ntrs.nasa.gov/citations/20250003104].

[15] T. Tallerico, A. D. Anderson, and J. J. Scheidler, "Concept design of a 5 MW axial flux partially superconducting electric machine," AIAA Aviation Forum & ASCEND, AIAA 2024-4092, Las Vegas, NV, 2024.

[16] K. Halbach, "Design of permanent multipole magnets with oriented rare Earth cobalt materials," Nucl. Instrum. Methods, vol. 169, no. 1, 1980.

[17] K. Halbach, "Applications of permanent magnets in accelerators and electron storage rings," J. Appl. Phys., vol. 57, no. 1, 1985.

[18] D. Ao, Y. Li, and C. Liu, "A review of cavitation problems of cryogenic fluids in gathering pipelines," J. Pipeline Sci Eng., vol. 5, no. 4, 100269, 2025.

APPENDIX

The Helmholtz motor is a patent pending electric machine that enables the use of high temperature superconductor (REBCO) in the stator winding by optimizing the magnetic field applied to the superconductor to minimize AC loss in it. This is achieved by locating the stator between a pair of rotors that rotate together and act like a collection of Helmholtz coil pairs to produce a nearly unidirectional magnetic field in the stator. The superconducting coils are constructed so that the quasi-unidirectional field acts in or very near the plane of the superconductor. A schematic of a radial flux Helmholtz motor is depicted in Fig. 7.

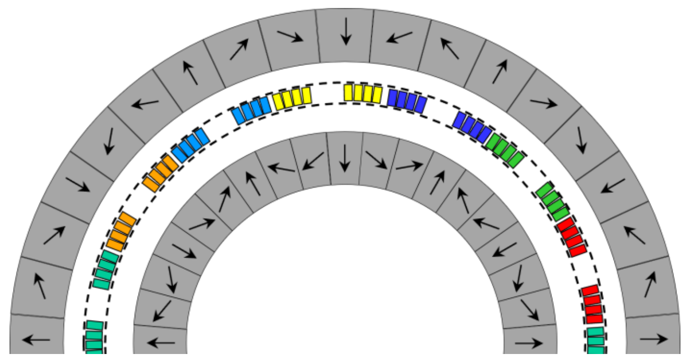

Fig. 7 Schematic cross section of an example radial flux Helmholtz machine with a concentrated HTS stator winding having 14 slots and 12 poles.